

Short Communication

Facile Synthesis of a High-Capacity $\text{LiNi}_{0.8}\text{Co}_{0.15}\text{Al}_{0.05}\text{O}_2$ Nanoplate Cathode with a {010} Orientation for Lithium-ion Batteries

Qi Wang, Lei Zhang*, Pengduo Zhao, Zhipeng Du

Naval Research Academy, Beijing 100000, China.

*E-mail: KCJXZH6@163.com.

Received: 5 July 2018 / Accepted: 16 August 2018 / Published: 1 October 2018

Ni-rich cathode $\text{LiNi}_{0.8}\text{Co}_{0.15}\text{Al}_{0.05}\text{O}_2$ nanoplates (NCA-NPs) are controlled synthesized using a facile and versatile method. The solvent (ethylene glycol) is very crucial for the formation of NCA-NPs which have exposed {010} electrochemically active planes. Applied in a lithium ion battery as the cathode, the NCA-NP sample sintered at 750 °C for 12 h demonstrates a high specific discharge capacity and an excellent rate capability, which can be attributed to the distinctive structures of the nanoplates with exposure to the {010} planes.

Keywords: Cathodes; Controlled synthesis; $\text{LiNi}_{0.8}\text{Co}_{0.15}\text{Al}_{0.05}\text{O}_2$; Lithium-ion batteries; {010}-oriented nanoplates

1. INTRODUCTION

Recently, nickel-rich layered oxides have drawn great attention as the cathode materials for hybrid electric vehicles (HEV) and electric vehicles (EV) with lithium-ion batteries (LIBs), owing to their high capacity, low cost and toxicity. [1,2] Among these layered materials, $\text{LiNi}_{0.8}\text{Co}_{0.15}\text{Al}_{0.05}\text{O}_2$ (NCA) has been successfully adopted in commercial LIBs. Nevertheless, several major drawbacks of NCA materials, especially drastic power fading at high discharge–charge rates, prevent its large-scale use as a cathode material in LIBs. [3,4]

It is well known that the morphological and surface microstructures are critical to the Li^+ transportation of electrode materials. [5] Recently, considerable efforts have been made for the synthesis of nanostructured NCA materials with different morphologies, to enhance their rate capabilities and cycle lives. Yang H. et al. synthesized yolk–shell NCA microspheres with a high discharge capacity and a good cyclic performance via an ultrasonic atomization method. [6] Wu N. et

al. fabricated one-dimensional NCA microrods with excellent electrochemical performance by a co-precipitation method. [7] In addition, NCA as an α -NaFeO₂ layered structure has a two-dimensional Li⁺-ion diffusion tunnel, in which Li⁺-ions transport along the a (or b) axis. The tunnels include the (010), (0 $\bar{1}$ 0), (100), (110), (1 $\bar{1}$ 0) and ($\bar{1}$ 00) planes denoted as {010} facets, which are parallel to the Li⁺-ion layers. NCA nanoplates with exposed {010} active planes exhibit more Li⁺-ion charge transfer reaction sites. Therefore, these additional reaction sites can help to improve the electrochemical performance, especially the rate capability. Wang Z. et al. obtained hierarchical NCA plates with exposed {010} active planes via a solvothermal method. [4] However, the synthesis of NCA with {010}-oriented plates through a facile method to decrease costs is also a challenge.

Herein, NCA nanoplates (NCA-NP) with controlled growth of the {010} planes were obtained by using a facile and versatile method, in which ethylene glycol is used not only as a solvent but also as a chelating reagent.

2. EXPERIMENTAL

2.1 Preparation of NCA-NP

All the reagents were purchased and without further purification. According to a molar ratio of 10.5:8:1.5:0.5, LiCH₃COO, Ni(CH₃COO)₂·6H₂O, Co(CH₃COO)₂·4H₂O and Al(NO₃)₃·9H₂O were dissolved in an appropriate amount of ethylene glycol with a total metal ion concentration of 0.05 M. Then, the solution was stirred to ensure that all the solid dissolved. After maintaining the solution at 85 °C for 8 h, it was placed into an air dry oven to obtain a fluffy precursor. The precursor was carefully ground to a fine powder with a mortar and pestle. Finally, the fine powder was pre-heated at 450 °C for 5 h and calcined at 700, 750 and 800 °C for 6, 12 and 18 h under an oxygen atmosphere, respectively. In addition, the samples are denoted as NCA-700C12h, NCA-750C12h, NCA-800C12h, NCA-750C6h and NCA-750C12h.

2.2. Characterization of the NCA-NPs

The structures of the NCA-NP samples were characterized by powder X-ray diffraction (XRD), which was performed on a PANalytical X-pert diffractometer (PANalytical, Netherlands) with Cu K α radiation from 10° to 80° at a voltage of 40 kV and a current of 40 mA at room temperature. The morphologies and microstructures of the NCA-NP samples were determined using the SEM and TEM images obtained from the S-4800 and JEM-2100. The results of ICP-AES were recorded by ICAP-6300.

2.3. Electrochemical measurements of the NCA-NP cathode

The electrochemical performance of the NCA-NP samples were measured by CR2025 coin cells with a lithium metal anode in an argon-filled glove box. The fabrication of the electrodes are

shown the literature. [5] The NCA-NP sample as the active material, carbon black as the conductive reagent and poly(vinylidene fluoride) (PVDF) as a binder were mixed (8:1:1 wt%) in N-methyl-2-pyrrolidone (NMP) to form a slurry. The slurry was transferred to aluminum foil and then dried in a vacuum oven. Finally, the cells were fabricated in an argon-filled glove box (with $O_2 < 1$ ppm and $H_2O < 1$ ppm). Celgard 2400 films were used as the separators. The electrolyte was a solution of 1 M $LiPF_6$ dissolved in ethyl carbonate/dimethyl carbonate/diethyl carbonate (EC/DMC/DEC) (1:1:1 v/v/v). The loading mass of the NCA-NP active material in one electrode was approximate 2 mg cm^{-2} . Galvanostatic charge-discharge testing was performed at different current densities between 2.7 and 4.3 V on a LAND CT-2001A cell test instrument. Cyclic voltammetry (CV) was conducted on a CHI660E electrochemical workstation between 2.7 and 4.3 V at a scan rate of $0.1\text{--}0.7 \text{ mV s}^{-1}$. Electrochemical impedance spectroscopy (EIS) measurements were carried out with a CHI660E electrochemical workstation between 100 kHz and 0.01 Hz with an AC signal of 5 mV.

3. RESULTS AND DISCUSSION

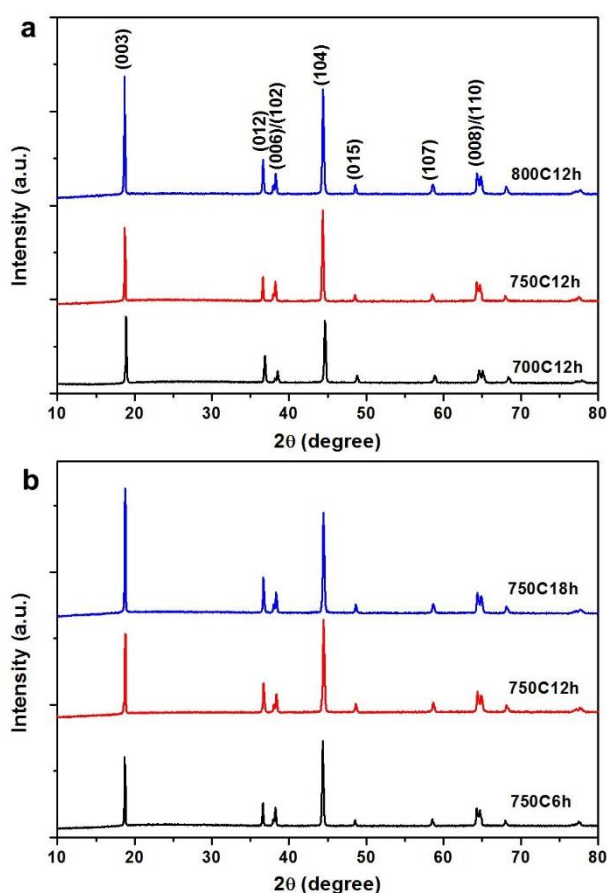


Figure 1. XRD patterns of the NCA-NP material: (a) different sintering temperatures; and (b) different sintering times.

Layer transition metal oxide nanoplates can be controlled fabricated with ethylene glycol owing to its bi-functional groups. [5,8,9] The reaction with metal ions generates a plate-like structure

through the hydrogen bond and chelating effects, which leads to a slowing of the nucleation along the width orientation. The process leads to a {010}-oriented NCA nanoplates.

Figure 1 shows the XRD patterns of the NCA-NP material synthesized at different sintering temperatures and times. All the samples show sharp peaks indexed with an α -NaFeO₂ structure (space group: R-3m). The clear separations of the adjacent peaks of (006)/(102) and (108)/(110) indicate to a typical layered structure. Specially, the intensities of the (003) peaks are lower than those of the (104) peaks under lower sintering temperature and shorter time conditions, which can result from a nanoplate morphology with special facets. [5] The observation is in accordance with the SEM and TEM results. The ICP-AES results (Table S1 in the Supplementary Materials) show that the exact molar ratio of the metal ions in the NCA-NP materials are consistent with the expected stoichiometry within experimental errors.

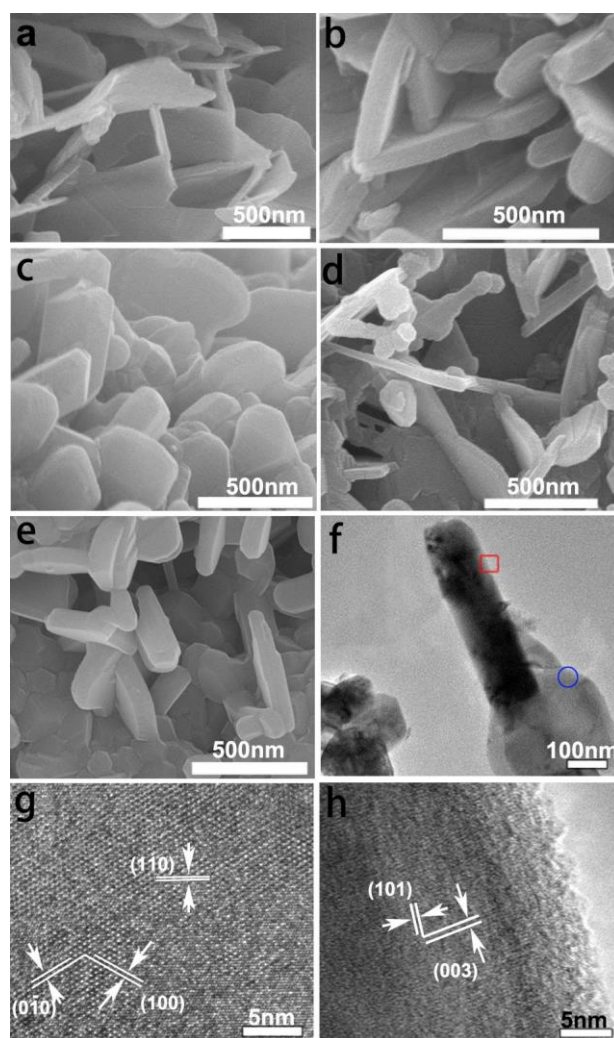


Figure 2. (a-e) SEM images of the NCA-NP samples under at different sintering conditions: (a) 700 °C, 12 h; (b) 750 °C, 12 h; (c) 800 °C, 12 h; (d) 750 °C, 6 h; (e) 750 °C, 18 h. (f-h) TEM and HRTEM images of the sample sintered at 750 °C for 12 h; (g) front view of the nanoplate (the round region in f); (h) lateral view of the nanoplate (the square region in f).

Figure 2 shows the SEM, TEM and HRTEM images of all the NCA-NP samples. From the SEM and TEM images, all the samples show a nanoplate morphology with a good dispersivity. Notably, the thickness increases with increasing sintering temperature and time. To further characterize the morphology and structure, TEM was conducted for the NCA-NP sample sintered at 750 °C for 12 h (NCA-750C12h).

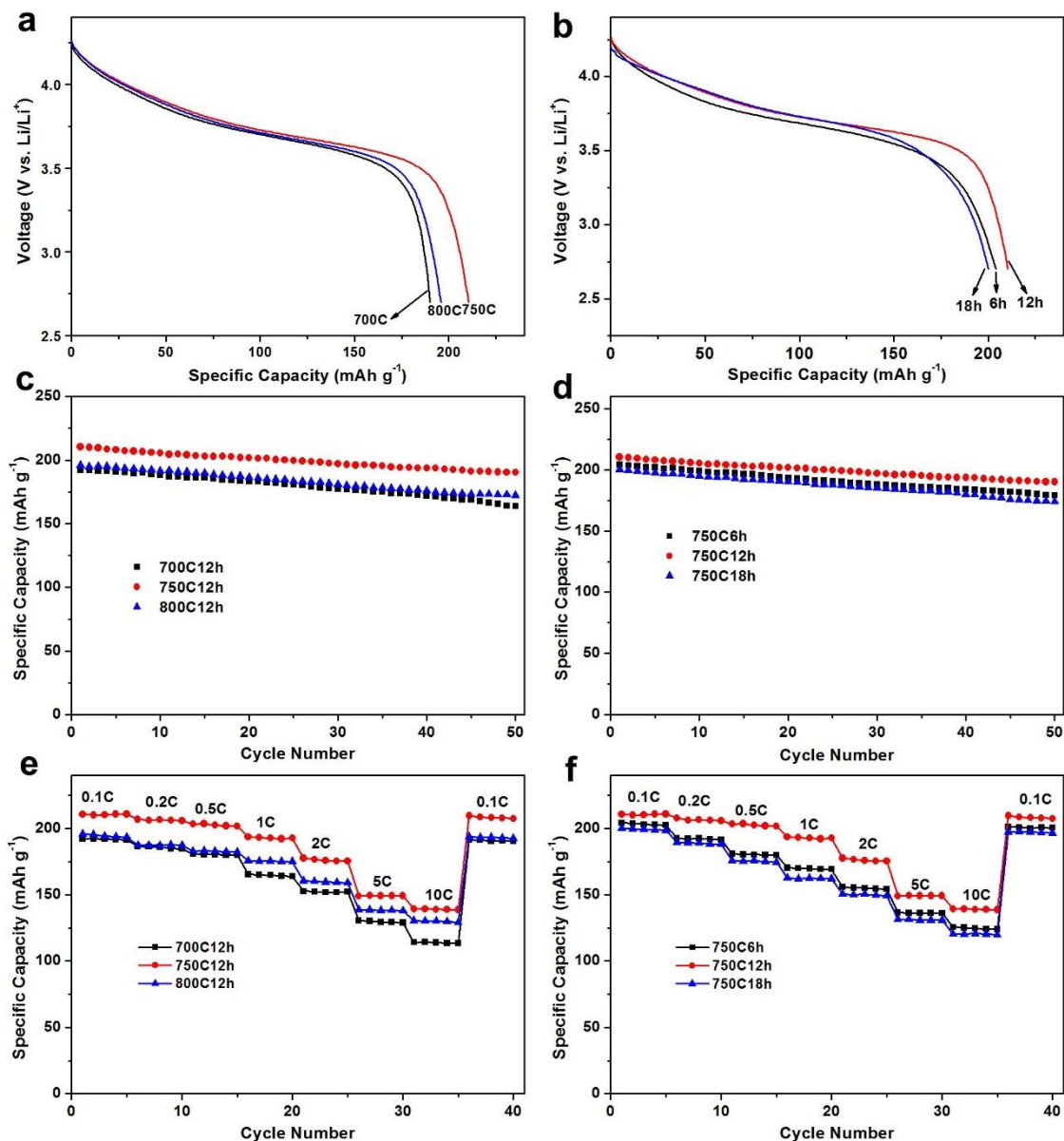


Figure 3. (a,b) The first discharge curves of NCA-NP at 0.1C between 2.7 and 4.3 V. (c,d) The cycle life of the NCA-NP samples. (e,f) The rate capability of the NCA-NP samples.

Figure 2g and h show the structure of the samples from the front and lateral views. There are three sets of lattice fringes in Figure 2g. The two fringes with same interplanar distance are measured to be 2.46 Å and are assigned to the (0 $\bar{1}$ 0) and (100) planes, respectively. The one fringe has a different *d* spacing (1.43 Å) and belongs to (110) planes. From the lateral view (Figure 2h), there are two sets of lattice fringes with interplanar distances measured to be 4.75 Å and 2.44 Å, which correspond to the

(003) and (101) planes, respectively. Based on the above analysis, the top and bottom planes are the electrochemically inert {001} facets, and the lateral plane belongs to the electrochemically active {010} facets. [4,5]

Figure 3 shows the electrochemical performance for the NCA-NP cathodes between 2.7 and 4.3 V at different current densities (1 C = 180 mA g⁻¹). The NCA-750C12h sample exhibits the highest discharge capacity of 210.4 mAh g⁻¹ with an 88.1% coulombic efficiency during the first cycle at a 0.1 C rate. After 50 charge/discharge cycles, the NCA-750C12h sample also shows excellent stability with a 90% of capacity retention, which is obviously higher than the retention of the other samples (Table 1). Figure 3e-f show the rate capability of the NCA-NP material cathode tested from 0.1 to 10 C. Notably, the discharge capacity can be up to 139.3 mAh g⁻¹ at 10 C for the NCA-750C12h cathode, which is the best rate performance. Compared with the NCA samples reported in the literatures (Table 2), [3,4,6,7,10] the NCA-NP cathodes display excellent electrochemical performance. The superior electrochemical performance of the NCA-NP cathode can be mainly attributed to the special nanoplate structure with exposed {010} active facets. [4] The exposure of the {010} active facets can provide more channels for Li⁺-ion transportation. [4,5] The NCA {010}-oriented nanoplates sintered at 750 °C for 12 h demonstrate superior electrochemical performance owing to the unique morphology and structure. The nanoplates can provide a short diffusion distance for the Li⁺-ions. The special {010} orientation can provide more electrochemical reaction active sites.

Table 1. The electrochemical performance of the NCA-NP samples.

| Sample | 0.1 C /Capacity (mAh g ⁻¹) | | Current density /Capacity (mAh g ⁻¹) | | | | | |
|--------------------|--|-----------|--|-------|-------|-------|-------|-------|
| | Charge | Discharge | 0.2 C | 0.5 C | 1 C | 2 C | 5 C | 10 C |
| NCA-700C12h | 220.5 | 192.3 | 185.5 | 180.8 | 165.4 | 152.7 | 130.5 | 114.2 |
| NCA-750C12h | 238.9 | 210.4 | 207.8 | 203.3 | 193.7 | 177.7 | 149.2 | 139.3 |
| NCA-800C12h | 224.3 | 195.8 | 187.5 | 183.0 | 175.6 | 160.4 | 138.8 | 130.5 |
| NCA-750C6h | 236.1 | 204 | 192.7 | 181.0 | 170.4 | 155.9 | 136.3 | 125.6 |
| NCA-750C18h | 233.4 | 200.1 | 189.5 | 175.8 | 162.7 | 150.5 | 131.6 | 120.6 |

Table 2. Comparison of the electrochemical performance of NCA-NP with reported results.

| Sample | Current density/Capacity (mAh g ⁻¹) | | | | | | Ref. |
|-----------------------|---|-------|-------|-------|-------|-------|----------|
| | 0.2 C | 0.5 C | 1 C | 2 C | 5 C | 10 C | |
| NCA-750C12h | 207.8 | 203.3 | 193.7 | 177.7 | 149.2 | 139.3 | our work |
| NCA | ~185 | ~175 | 169.1 | ~155 | ~135 | / | 3 |
| HP-NCA | / | 179 | 165 | 154 | 138 | 124 | 4 |
| yolk-shell NCA | ~205 | ~185 | 129.7 | / | / | / | 6 |
| NCA-MRs | 200 | 181 | 172 | 159 | 137 | 115 | 7 |
| CD-NCA | ~155 | 135.9 | ~105 | 107.6 | / | / | 10 |

Cyclic voltammetry (CV) curves for the NCA-NP sample obtained from sintering at 750 °C for 12 h are shown in Figure S1. All the CV curves illustrate the phase transition process between the H1 and H3 phase, in which the strongest peak at approximately 3.85/3.67 V is assigned to the phase transition reaction of the H1 and M phases. [10] With an increasing scan rate, the peak intensity and site are larger for the NCA-NP cathode with the same results for all electrodes. In addition, the calculated Li⁺-ion diffusion constant D_{Li} is 1.06×10^{-11} cm² s⁻¹ from the results of CV, which is larger than that of most of the NCA cathodes.[11] The fast diffusion of the Li⁺-ions illustrates the excellent rate capability.

To gain further insight into the electrochemical behavior, EIS measurements were carried out for all the NCA samples as the working electrodes. As seen from the Nyquist plots (Figure S2), all the NCA samples exhibit high-frequency semi-circles and inclined lines, which represent different physical significances. [4] Among all the samples, the NCA-NP material obtained at 750 °C for 12 h shows the smallest charge transfer and a solid-electrolyte interface impedance of 57.8 Ω leading to a superior rate capability.

4. CONCLUSIONS

In summary, layered Ni-rich NCA nanoplates with exposed {010} electrochemical active planes are successfully synthesized via a facile method. As the cathode for LIB, the NCA-NP material obtained at 750 °C for 12 h displays excellent electrochemical performance with a high specific discharge capacity and a superior rate capability. These characteristics can be due to the distinctive structure with the exposure of more {010} electrochemically active planes.

References

1. S.-T. Myung, F. Maglia, K.-J. Park, C. S. Yoon, P. Lamp, S.-J. Kim and Y.-K. Sun, *ACS Energy Lett.*, 2 (2017), 196.
2. W. Liu, P. Oh, X. Liu, M. J. Lee, W. Cho, S. Chae, Y. Kim and J. Cho, *Angew. Chem. Int. Ed.*, 54 (2015), 4440.
3. L. Zhu, Y. Liu, W. Wu, X. Wu, W. Tang and Y. Wu, *J. Mater. Chem. A*, 3 (2015), 15156.
4. Z. Wang, H. Liu, J. Wu, W.-M. Lau, J. Mei, H. Liu and G. Liu, *RSC Adv.*, 6 (2016) 32365.
5. J. Li, R. Yao, and C. Cao, *ACS Appl. Mater. Interfaces*, 6 (2014) 5075.
6. H. Z. Yang, P. X. Liu, Q. L. Chen, X. W. Liu, Y. W. Lu, S. F. Xie, L. Ni, X. Y. Wu, M. Y. Peng, Y. B. Chen, Y. F. Tang and Y. F. Chen, *RSC Adv.*, 4 (2014) 35522.
7. N. T. Wu, H. Wu, W. Yuan, S. J. Liu, J. Y. Liao and Y. Zhang, *J. Mater. Chem. A*, 3 (2015) 13648.
8. J. Li, T. Jia, K. Liu, J. Zhao, J. Chen, C. Cao, *J. Power Sources*, 333 (2016) 37.
9. J. Li, C. Xu, J. Zhao, J. Chen, C. Cao, *J. Alloy. Compd.*, 734 (2018) 301.
10. Y. Chen, P. Li, S. Zhao, Y. Zhuang, S. Zhao, Q. Zhou and J. Zheng, *RSC Adv.*, 7 (2017) 29233.
11. J. Li, L. Wan, and C. Cao, *Electrochim. Acta*, 191 (2016) 974.

© 2018 The Authors. Published by ESG (www.electrochemsci.org). This article is an open access article distributed under the terms and conditions of the Creative Commons Attribution license (<http://creativecommons.org/licenses/by/4.0/>).